

## Study on the Dynamic Instability of a Bus in Crosswind Conditions

*Minh Hoang Trinh\**, *Tien Quyet Do*, *Trong Hoan Nguyen*

*Hanoi University of Science and Technology, Hanoi, Vietnam*

*\*Email: hoang.trinhminh@hust.edu.vn*

### Abstract

*When a grand bus moves on the road, aerodynamic forces and moments can be the leading cause of vehicle instability and accidents. Therefore, studying the influence of aerodynamic forces and moments on the instability of grand buses is a matter of concern. This article investigates bus' safety when moving in crosswind conditions with three types of motion instability: loose contact, rollover, and sideslip. A static model is used to determine the speed limits when the vehicle is unstable. The basic equations are selected based on the assumption that the vehicle moves straight in the driving line on the road. The aerodynamic forces and moments are characterized by the aerodynamic coefficients determined by the bus's aerodynamic simulation model. The article has focused on determining the limit speeds of crosswinds that cause instability of the 45-seat bus by numerical method. The study results can be used as a basis for assessing the influence of aerodynamic forces on the dynamic instability of the bus during the movement on the road in complex windy conditions.*

Keywords: Crosswind, grand bus, instability, rollover, sideslip.

### 1. Introduction

For grand buses, due to the large surface area and long-distance travel, the risk of dynamic instability will increase when the car is moving in high crosswind conditions. It is necessary to determine the dangerous speed threshold to alert the driver. However, it is difficult and costly to determine the dynamic parameters when the vehicle moves in a high crosswind. Therefore, many studies have proposed determining the dangerous speed threshold during the operation of automobiles in different wind speed ranges (in static form).

One of the criteria for determining the probability of an accident when the vehicle moves in crosswind conditions proposed by Hucho [1]. He introduced the possible accident danger levels based on the evaluation of vehicle lateral displacement from the driving line during the first 0.8 seconds after the car moves into the crosswind area. Other criteria proposed by Barker [2]. According to him, crosswind accidents may be classified into three types: rollover, sideslip, and rotating accidents. Barker also proposed some criteria to evaluate the above types of accidents when the vehicle moves into the crosswind area, as follows:

- The contact force (vertical force) between the wheel and the road is reduced to zero in 0.5 s.
- The vehicle's lateral displacement exceeds 0.5 m within 0.5 s.
- The vehicle's yaw angle exceeds  $11.5^{\circ}$  (0.2 rad) within 0.5 s.

The vehicle stability in crosswind conditions depends on many factors such as vehicle specifications, driving conditions, crosswind characteristics, and driver reactions. However, driver reaction is a random process that is difficult to determine. Therefore, in most of the previous studies on lateral stability, the influence of the driver reaction is often not taken into account [3, 4].

The study of vehicle stability in crosswind conditions, in particular, has also been mentioned in a number of publications. The study of the vehicle dynamic instability under the influence of external factors (road, wind) usually is done by simulation method using dynamic models. However, this is a complicated problem because the aerodynamic characteristics of each vehicle are different. Therefore, some authors have proposed studies on the instability of some vehicles under static crosswind conditions. Some specific studies have been carried out to evaluate the influence of aerodynamic forces on the instability of passenger cars [2, 5], or trailers [6]. In fact, for each particular vehicle, the influence of aerodynamic forces and moments on vehicle stability is very different. Therefore, the study to determine their influence on bus instability is a significant problem in science and practice. This paper focuses on determining the wind speed limits causing instability of grand buses, using criteria of the crosswind accident [2, 5]. The criteria include the following:

- The contact force (vertical force) between the wheel and the road is reduced to zero (rollover

instability, Fig. 1a).

- The side force at all wheels exceeds the limit of lateral slip (sideslip instability, Fig. 1b).

- The side force at wheels in an axle exceeds the lateral slip limit (rotation instability, Fig. 1c).

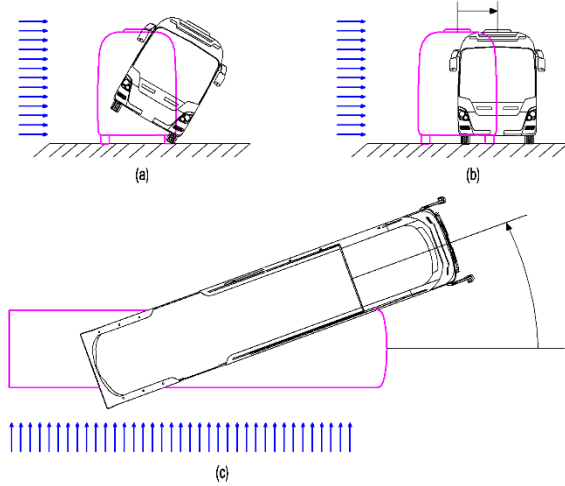


Fig. 1. Types of instability when the vehicle is moving in crosswind conditions

## 2. Determination of Contact Forces between the Wheels and the Road

A model of a two-axle bus is used for this case study. The bus is assumed to be a rigid body, which is characterized by mass and dimensions. Assume the bus moves in a straight line until instability occurs. In this study, no driver reaction was considered.

Fig. 2 presents the forces and moments acting on

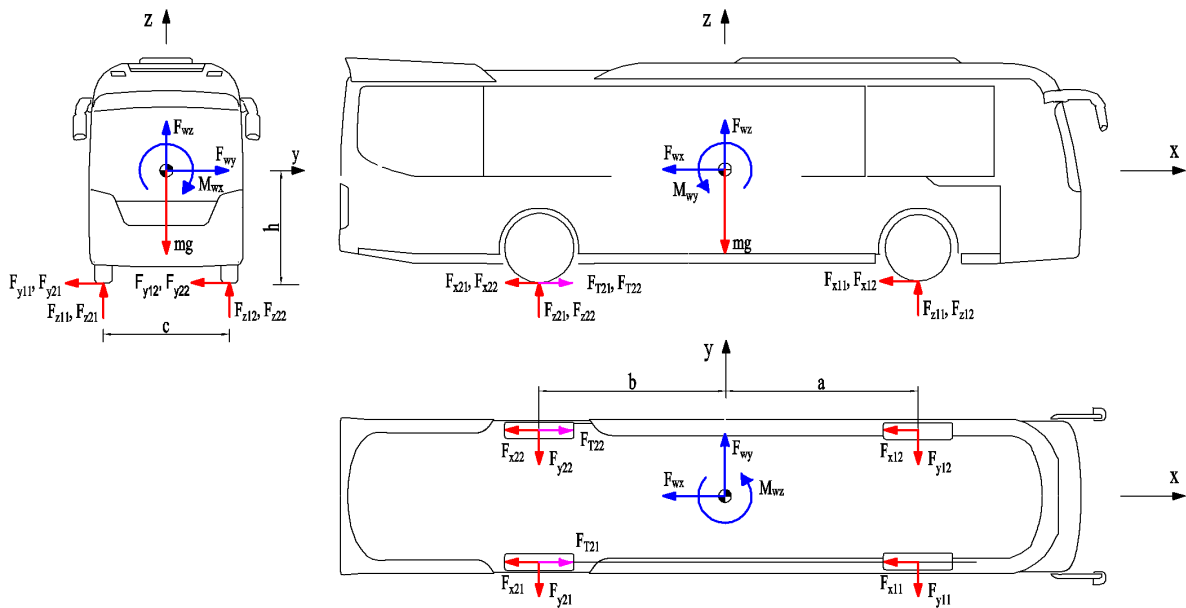


Fig. 2. Reaction forces and wind-induced resultant forces and moments on the vehicle.

the bus when moving in a straight line and crosswind conditions. When the bus is in motion, at the center of gravity (COG) of the bus, there are six equilibrium equations of force and moments, corresponding to three translational motions and three rotational motions. In this case, the Cartesian coordinate system is used to describe the motion of the bus. The origin is the COG of the bus; the  $x$ -axis is the longitudinal axis of the bus in the direction of motion; the  $y$ -axis is the transverse axis of the bus in the direction of the crosswind; The  $z$ -axis is the upward vertical axis.

The force equilibrium equations at the COG of the bus (in the three  $x$ ,  $y$ , and  $z$  axes, respectively) are as follows:

$$-F_{wx} - F_{x11} - F_{x12} - F_{x21} - F_{x22} + T_{21} + T_{22} = 0 \quad (1)$$

$$-F_{wy} - F_{y11} - F_{y12} - F_{y21} - F_{y22} = 0 \quad (2)$$

$$-mg + F_{wz} + F_{z11} + F_{z12} + F_{z21} + F_{z22} = 0 \quad (3)$$

The moments' equilibrium equations at the COG of the bus (in the three  $x$ ,  $y$ , and  $z$  axes, respectively) are:

$$-M_{wx} - \frac{c}{2}(F_{z11} - F_{z12} + F_{z21} - F_{z22}) \quad (4)$$

$$-h(F_{y11} + F_{y12} + F_{y21} + F_{y22}) = 0$$

$$-M_{wy} - a(F_{z11} + F_{z12}) + b(F_{z21} + F_{z22}) \quad (5)$$

$$+h(F_{x11} + F_{x12} + F_{x21} + F_{x22} - T_{21} - T_{22}) = 0$$

$$M_{wz} - a(F_{y11} + F_{y12}) + b(F_{y21} + F_{y22}) \quad (6)$$

$$+ \frac{c}{2}(F_{x12} - F_{x11} + F_{x22} - F_{x21} + T_{21} - T_{22}) = 0$$

where  $g$  is the Earth's gravity,  $m$  is the mass of the bus;  $a$ ,  $b$  is the distance from the front and rear axle to the COG of the bus;  $c$  is the track width;  $h$  is the vertical distance from COG of the bus to the ground.

A system of six equilibrium equations includes 20 components of forces and moments: six aerodynamic forces and moments are: drag force  $F_{wx}$ , side force  $F_{wy}$ , lift force  $F_{wz}$ , rolling moment  $M_{wx}$ , pitching moment  $M_{wy}$ , and yawing moment  $M_{wz}$ ; 12 reaction forces are 4 tire rolling resistance forces  $F_{xij}$ , 4 tire side friction forces  $F_{yij}$ , and 4 wheel loads  $F_{zij}$  ( $i = 1, 2$  and  $j = 1, 2$ ); and two tire traction forces at the rear wheels ( $T_{21}$ ,  $T_{22}$ ). These forces are determined as described below.

Let  $(x_{ij}, y_{ij}, z_{ij})$  be coordinates of the center of the  $ij$ th wheel of the bus. Because the vehicle is assumed to be a rigid body, all wheel's centers must lie in one plane. Hence we have a constraint equation:

$$z_{11} - z_{12} + z_{22} - z_{21} = 0 \quad (7)$$

If we assume that the loads  $F_{zij}$  at each wheel is proportional to the displacement  $z_{ij}$  and the stiffness of the suspension is the same at all wheels, then (7) is converted to the constraint equation:

$$F_{z11} - F_{z12} - F_{z21} + F_{z22} = 0 \quad (8)$$

The condition of the wheel's contact with the road surface is  $F_{zij} \geq 0$ . If  $F_{zij} = 0$ , the wheel will lose contact with the road surface.

Assume that when the vehicle is stable, the longitudinal and transverse reactions are within the limited frictional forces determined by Coulomb friction law. If we further assume that the limit of friction is the same in all directions, then at each wheel, there is a constraint equation between the reaction components as follows:

$$\sqrt{(T_{ij} - F_{xij})^2 + F_{yij}^2} \leq \mu F_{zij} \quad (9)$$

where  $\mu$  is the friction coefficient. The tire rolling resistance of the wheel is calculated as follows:

$$F_{xij} = fF_{zij} \quad (10)$$

where  $f$  is the tire rolling coefficient [7]. In this study, rolling resistance is assumed to be the same for all wheels.

Assume the traction force at the wheels is proportional to the vertical reaction at each rear wheel.

$$T_{ij} = qF_{zij} \quad (11)$$

where  $q$  is the traction coefficient. The traction coefficient is also assumed to be the same for all rear wheels (driven wheel).

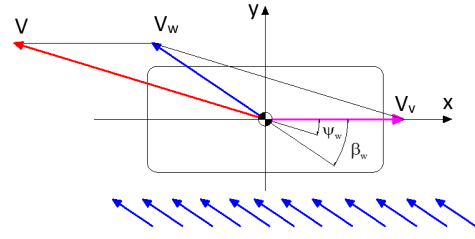


Fig. 3. Equivalent wind speed when the vehicle is moving in crosswind conditions

When the vehicle moves with absolute speed  $V_v$  in the condition of crosswind, which is characterized by a wind speed  $V_w$  and an angle  $\beta_w$  formed by the wind direction and the longitudinal direction ( $x$ -axis) of the bus, the effect of the crosswind, in this case, is the same as that of an equivalent wind acting on a stationary vehicle. This equivalent wind is characterized by a velocity  $V$  and an angle  $\psi_w$  with the longitudinal  $x$ -axis of the bus (Fig. 3).

According to the geometric relation in Fig. 3, we have:

$$V^2 = (V_v + V_w \cos \beta_w)^2 + V_w^2 \sin^2 \beta_w \quad (12)$$

$$\psi_w = \arctan \frac{V_w \sin \beta_w}{V_v + V_w \cos \beta_w} \quad (13)$$

In the condition of moving with the equivalent wind, the aerodynamic forces and moments acting on the bus COG then are calculated as follows:

$$\begin{aligned} F_{wx} &= C_x A \frac{\rho V^2}{2}; F_{wy} = C_y A \frac{\rho V^2}{2}; \\ F_{wz} &= C_z A \frac{\rho V^2}{2}; M_{wx} = C_{Mx} A h \frac{\rho V^2}{2} \\ M_{wy} &= C_{My} A h \frac{\rho V^2}{2}; M_{wz} = C_{Mz} A h \frac{\rho V^2}{2} \end{aligned} \quad (14)$$

where  $C_x$ ,  $C_y$ ,  $C_z$ ,  $C_{Mx}$ ,  $C_{My}$ ,  $C_{Mz}$ , are the coefficients of aerodynamic forces and aerodynamic moments corresponding to the coordinate axes.  $A$  is the characteristic area of the vehicle, which is usually taken as the projection of the vehicle's front area.  $h$  is the vertical distance from the COG of the bus to the ground,  $\rho$  is the air density.

Because the large bus is assumed to be a rigid body, when a side force is applied, the wheel may slide in the side direction. Therefore, the tire side friction forces at each wheel are calculated as follows:

$$F_{y1j} = s_1 F_{z1j}; \quad F_{y2j} = s_2 F_{z2j} \quad (j = 1, 2) \quad (15)$$

where  $s_1$  and  $s_2$  are the sideslip parameters for the front and the rear wheels.

Thus, the system is left with only seven unknowns  $F_{z11}$ ,  $F_{z12}$ ,  $F_{z21}$ ,  $F_{z22}$ ,  $s_1$ ,  $s_2$ , and  $q$ . The system of equations is described as follows:

$$\begin{cases}
 -F_{wx} - f(F_{z11} + F_{z12} + F_{z21} + F_{z22}) + q(F_{z21} + F_{z22}) = 0 \\
 F_{wy} - s_1(F_{z11} + F_{z12}) - s_2(F_{z21} + F_{z22}) = 0 \\
 -mg + F_{wz} + F_{z11} + F_{z12} + F_{z21} + F_{z22} = 0 \\
 -M_{wx} - \frac{c}{2}(F_{z11} - F_{z12} + F_{z21} - F_{z22}) \\
 + h[s_1(F_{z11} + F_{z12}) + s_2(F_{z21} + F_{z22})] = 0 \\
 -M_{wy} - a(F_{z11} + F_{z12}) + b(F_{z21} + F_{z22}) \\
 + hf(F_{z11} + F_{z12} + F_{z21} + F_{z22}) - hq(F_{z21} + F_{z22}) = 0 \\
 M_{wz} + \frac{c}{2}q(F_{z22} - F_{z21}) - as_1(F_{z11} + F_{z12}) \\
 + bs_2(F_{z21} + F_{z22}) + \frac{c}{2}f(F_{z11} + F_{z12} - F_{z21} - F_{z22}) = 0 \\
 F_{z11} - F_{z12} + F_{z21} - F_{z22} = 0
 \end{cases} \quad (16)$$

Solving (16), we have:

$$\begin{cases}
 F_{z11} = \frac{1}{2} \left( \frac{b(mg - F_{wz})}{a+b} - \frac{hF_{wy} + M_{wx}}{c} - \frac{hF_{wx} + M_{wy}}{a+b} \right) \\
 F_{z12} = \frac{1}{2} \left( \frac{b(mg - F_{wz})}{a+b} + \frac{hF_{wy} + M_{wx}}{c} - \frac{hF_{wx} + M_{wy}}{a+b} \right) \\
 F_{z21} = \frac{1}{2} \left( \frac{a(mg - F_{wz})}{a+b} - \frac{hF_{wy} + M_{wx}}{c} + \frac{hF_{wx} + M_{wy}}{a+b} \right) \\
 F_{z22} = \frac{1}{2} \left( \frac{a(mg - F_{wz})}{a+b} + \frac{hF_{wy} + M_{wx}}{c} + \frac{hF_{wx} + M_{wy}}{a+b} \right) \\
 s_1 = \frac{(bF_{wy} + M_{wz}) - \left(\frac{q}{2} - f\right)(hF_{wy} + M_{wx})}{b(mg - F_{wz}) - (hF_{wx} + M_{wy})} \\
 s_2 = \frac{(aF_{wy} - M_{wz}) + \left(\frac{q}{2} - f\right)(hF_{wy} + M_{wx})}{a(mg - F_{wz}) + (hF_{wx} + M_{wy})} \\
 q = \frac{(a+b)[F_{wx} + f(mg - F_{wz})]}{a(mg - F_{wz}) + (hF_{wx} + M_{wy})}
 \end{cases} \quad (17)$$

From (17), the total tire side friction forces at each axle are:

$$F_{y11} + F_{y12} = \frac{bF_{wy} + M_{wz}}{a+b} - q' \frac{hF_{wy} + M_{wx}}{a+b} \quad (18)$$

$$F_{y21} + F_{y22} = \frac{aF_{wy} - M_{wz}}{a+b} + q' \frac{hF_{wy} + M_{wx}}{a+b} \quad (19)$$

where:

$$q' = \frac{q}{2} - f \quad (20)$$

The wheel loads  $F_{zij}$ , from (17) and the total tire side friction forces, from (18) and (19), will be used to evaluate the instability of the bus.

### 3. Case Studies of Instability

#### 3.1. Wheels Lose Contact with the Road

##### 3.1.1. One wheel loses contact with the road

When there is a crosswind from the right direction (Fig. 2), from (17), we have:

$$F_{z12} - F_{z11} = F_{z22} - F_{z21} = \frac{hF_{wy} + M_{wx}}{c} \quad (21)$$

These expressions are all positive because  $M_{wx}$  and  $F_{wy}$  are both positive. Therefore, if the vehicle overturns, the right wheels 11 and 21 will lose contact first. The limit speeds when wheel 11 or wheel 21 lose contact, respectively, can be determined as follows:

$$V_{loose11} = \sqrt{\frac{2mg}{\rho A} \frac{bc}{h(a+b)(C_y + C_{Mx}) + hc(C_x + C_{My}) + bcC_z}} \quad (22)$$

$$V_{loose21} = \sqrt{\frac{2mg}{\rho A} \frac{ac}{h(a+b)(C_y + C_{Mx}) - hc(C_x + C_{My}) + acC_z}} \quad (23)$$

##### 3.1.2. Rollover

The rollover condition specified in the references usually requires a vertical force applied to the wheels upwind, resulting in a simultaneous loss of contact with the road surface [2, 5]. Thus, the limit speed that causes the bus to roll around the left side (both right wheels lose contact):

$$V_{rollover} = \max(V_{loose11}, V_{loose21}) \quad (24)$$

#### 3.2. The Wheels Slip in the Side Direction

##### 3.2.1. Rotation

When the vehicle is rotated, the lateral force applied to each wheel exceeds the friction limit. From (15), the conditions for the front wheels and for the rear wheels to reach the sideslip are:

$$F_{y11} + F_{y12} = \mu_1(F_{z11} + F_{z12}) \quad (25)$$

$$F_{y21} + F_{y22} = \mu_2(F_{z21} + F_{z22}) \quad (26)$$

where  $\mu_1 = \sqrt{\mu^2 - f^2}$  ;  $\mu_2 = \sqrt{\mu^2 - (q-f)^2}$

Substituting the aerodynamic forces and moments from equations (1) to (6) into equations (25) and (26), the limit speeds causing sideslip at the wheels at each axis are determined as follows:

$$V_{Slip1} = \sqrt{\frac{2mg}{\rho A} \frac{\mu_1 b}{bC_y + h[C_{Mz} - q'(C_y + C_{Mx})] + \mu_1 [bC_z + h(C_x + C_{My})]}} \quad (27)$$

$$V_{Slip2} = \sqrt{\frac{2mg}{\rho A} \frac{\mu_2 a}{aC_y - h[C_{Mz} - q'(C_y + C_{Mx})] + \mu_2 [aC_z - h(C_x + C_{My})]}} \quad (28)$$

Here, the traction coefficient  $q$  in (17) will be calculated according to the aerodynamic coefficients as follows:

$$q = \frac{(a+b) \left[ C_x + f \left( \frac{2mg}{\rho AV^2} - C_z \right) \right]}{a \left( \frac{2mg}{\rho AV^2} - C_z \right) + h(C_x + C_{My})} \quad (29)$$

### 3.2.2. Sideslip

The criterion for sideslip is taken into account when all wheels simultaneously reach the friction limit. Therefore, the limit speed for the bus to completely sideslip is:

$$V_{sideslip} = \max(V_{Slip1}, V_{Slip2}) \quad (30)$$

### 3.3. Determination of Limit Speed that Causes Instability

When one of the unstable conditions mentioned in sections 3.1 and 3.2 occurs, there is a potential risk of causing an accident on the bus. Therefore, the determination of the limit speed that does not cause any instability in the above four cases will be significant in assessing the safety limit of the vehicle in crosswind conditions. In this study, the stability limit speed  $V_{stable}$  is determined as follows:

$$V_{stable} = \min(V_{loose11}, V_{loose21}, V_{Slip1}, V_{Slip2}) \quad (31)$$

## 4. Results and Discussion

### 4.1. Determination of Aerodynamic Coefficient by CFD Software

To calculate the limit speeds mentioned above, we need to determine the coefficients of aerodynamic forces and moments in the cases of vehicle movement with speed  $V_v$  and in wind conditions with speed  $V_w$  (according to the angle  $\psi_w$ ). Previous researchers often used a mathematical function to describe the dependence between these aerodynamic coefficients and the angle  $\psi_w$ . These mathematical functions are usually calculated by the interpolation method, based on the discrete values of the aerodynamic coefficient in some cases of the angle  $\psi_w$  for a specific vehicle. These aerodynamic coefficients are calculated by a CFD software. Some mathematical functions have been proposed, such as exponential function, trigonometric function [2, 5], or polynomial function of order 2 [6]. The determination of the mathematical function that characterizes the aerodynamic coefficient from the discrete values in the paper also uses the polynomial interpolation method. To evaluate the accuracy of the interpolation process to determine the aerodynamic coefficient, Zhang [6] used the R-square index (roots mean squared) with the criterion  $R\text{-square} > 0.95$ . It is also a good idea for the authors in this paper to determine the aerodynamic force and moment coefficients for the bus.

#### 4.1.1. Model for determining aerodynamic coefficients of 45-seat bus

This study was conducted with a 45-seat bus manufactured and assembled in Vietnam (Fig. 4). In the process of performing calculations by simulation method, in order to ensure the reliability of the model but suitable for computer memory, the model is set up with the following assumptions:

- The body model is rigid, regardless of tire deformation during the simulation;
- Model does not take into account the heat exchange process between the bus body and the air;
- The body surface is smooth, and the underbody is wrapped flat (ignoring the influence of other car details such as glass, wipers, door handles, etc.).

The 3-D model of the 45-seat bus body was built using Solidworks software (Fig. 4). The coordinate system during the aerodynamic simulation is the Cartesian coordinate system, with the origin located at the center of gravity of the bus.

The 45-seat bus model was then used to determine the aerodynamic coefficients using Ansys Fluent software. According to the simulation experience given in the Ansys Fluent software manual and according to some other authors [8], the airbox surrounding the body of the bus in this simulation is a rectangular box. The meshing in the simulation is performed differently in 3 airboxes: the first airbox closest to the vehicle is rectangular with dimensions: *length x width x height* = 15000 mm x 6000 mm x 4500 mm; The second airbox is also rectangular with dimensions: *length x width x height* = 30000 mm x 16000 mm x 10000 mm and the third airbox is far from the bus body (Fig. 5). Because the 45-seat bus body profile is very complex, the first airbox has meshed very finely, the second airbox is divided relatively finely, and the third airbox has meshed with large steps. After meshing, the model has 558293 nodes and 2354550 elements.

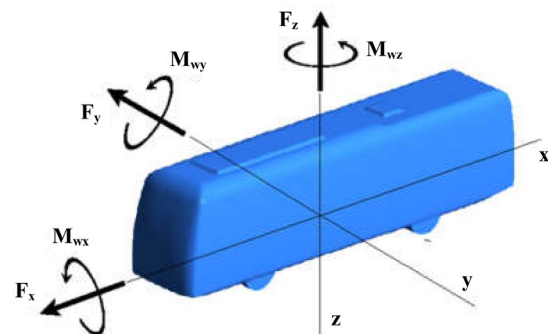


Fig. 4. 3D model of 45-seat bus and coordinate system

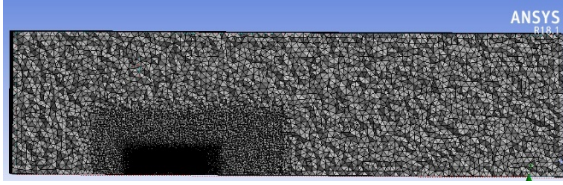


Fig. 5. Meshing the airbox to determine the aerodynamic coefficients in Ansys Fluent

In the study of automotive aerodynamics, researchers often use the Navier- Stoke equation to describe the flow of air around the bus body. In this study, the authors have chosen the k-epsilon model with the boundary condition as "Non-Equilibrium Wall Functions Wall Treatment" [9].

#### 4.1.2. Results of determination of aerodynamic force and moment coefficients

The aerodynamic coefficients are calculated using Ansys Fluent software and verified experimentally [10, 11]. In the model of calculating the aerodynamic coefficients, assuming the bus is stationary, a wind has velocity  $V_w$ , and the wind is inclined at an angle  $\beta_w$  to the longitudinal axis of the bus. Thus, in this case, the equivalent wind speed in this calculation  $V = V_w$  and  $\psi_w = \beta_w$ . The aerodynamic coefficients in each case of angle  $\psi_w$  calculated by Ansys Fluent software are shown in Table 1.

As mentioned in section 2, the change of the vehicle speed  $V_V$ , either of the speed  $V_w$  or the angle  $\beta_w$  of the wind, will change the equivalent wind parameters (wind speed  $V$  and impact angle  $\psi_w$ ). Therefore, it is necessary to define interpolation functions to calculate the aerodynamic coefficients as input parameters of the calculation model. From the results as the discrete values of the aerodynamic coefficients (Table 1), we have built a function of polynomials of order 4 to describe the dependence of the aerodynamic coefficients on the angle  $\psi_w$  of the equivalent wind.

Table 1. The aerodynamic coefficients corresponding to the angle  $\psi_w$

$\psi_w(^{\circ})$	Aerodynamic coefficients					
	$C_x$	$C_y$	$C_z$	$C_{Mx}$	$C_{My}$	$C_{Mz}$
0	0.51	0.00	-0.18	0.00	-0.12	0.00
10	0.65	0.97	0.13	0.04	0.03	0.28
20	0.69	1.91	0.77	0.06	0.03	0.53
30	0.61	2.93	1.37	0.08	0.02	0.64
40	0.44	3.88	1.67	0.12	-0.04	0.66
50	0.17	4.54	1.75	0.17	-0.09	0.61
60	-0.12	4.61	1.60	0.20	-0.08	0.55
70	-0.25	4.30	1.11	0.21	-0.05	0.32
80	-0.27	4.13	0.74	0.22	-0.05	0.04
90	-0.23	4.06	0.62	0.28	-0.07	-1.40

#### a. Aerodynamic force coefficients

The aerodynamic force coefficients calculated directly from the aerodynamic simulation model and calculated from the polynomial interpolation function of order 4 are shown in Fig. 6. The red square points represent the drag coefficient  $C_x$  calculated by direct simulation ( $C_{x,sim}$ ), and the red solid line represents the drag coefficient  $C_x$  calculated by the interpolation function ( $C_{x,fit}$ ). The blue circle points represent the side coefficient  $C_y$  calculated by direct simulation ( $C_{y,sim}$ ), and the blue dotted line represents the side coefficient calculated by the interpolation function ( $C_{y,fit}$ ). The black triangular points represent the lift coefficient  $C_z$  calculated by direct simulation ( $C_{z,sim}$ ), and the black dashed line represents the lift coefficient calculated by the interpolation function ( $C_{z,fit}$ ). The interpolation functions of the aerodynamic force coefficients are determined as follows:

$$C_x = 0.4969\psi_w^4 + 0.01637\psi_w^3 - 2.386\psi_w^2 + 1.361\psi_w + 0.5093 \quad (32)$$

$$C_y = 4.274\psi_w^4 - 14.1\psi_w^3 + 11.15\psi_w^2 + 3.267\psi_w \quad (33)$$

$$C_z = 4.636\psi_w^4 - 14.31\psi_w^3 + 11.19\psi_w^2 + 0.3152\psi_w - 0.1758 \quad (34)$$

To evaluate the accuracy of the interpolation process to determine the aerodynamic force coefficients, in this paper, the authors also use the R-square index (with the criterion R-square > 0.95, [6]). The interpolation functions to calculate the coefficients  $C_x$ ,  $C_y$ , and  $C_z$  in the paper all have R-square indexes of approximately 0.99.

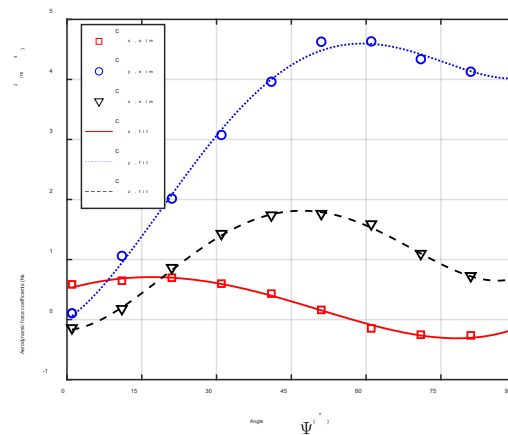


Fig. 6. Aerodynamic force coefficients

In fact, when the angle  $\psi_w = 0^{\circ}$ , the drag force  $F_{wx}$  only acts on the front surface of the bus. When the angle  $\psi_w$  is changed ( $0^{\circ} < \psi_w < 90^{\circ}$ ), aerodynamic forces appear on both the front and side surfaces of the bus, and thus the total longitudinal drag force  $F_{wx}$  may increase or decrease. Thus the drag coefficient  $C_x$  in these cases can be higher or lower than that when the angle  $\psi_w = 0^{\circ}$ . Similarly with the side force coefficient  $C_y$  can be higher or lower than that when angle

$\psi_w = 90^\circ$ . The results in Fig. 6 show that the drag coefficient reaches the maximum value  $C_{x,max} = 0.712$  at  $\psi_w = 16^\circ$ . The side coefficient reaches the maximum value  $C_{y,max} = 4,631$  at  $\psi_w = 58^\circ$ . The lift coefficient reaches the maximum value  $C_{z,max} = 1,803$  at  $\psi_w = 50^\circ$ .

*b. Aerodynamic moment coefficients*

The aerodynamic moment coefficients are shown in Fig. 7. The red square points represent the rolling coefficient  $C_{Mx}$  calculated by direct simulation ( $C_{Mx,sim}$ ), and the red solid line represents the rolling coefficient  $C_{Mx}$  calculated by the interpolation function ( $C_{Mx,fit}$ ). The blue circle points represent the pitching coefficient  $C_{My}$  calculated by direct simulation ( $C_{My,sim}$ ), and the blue dotted line represents the pitching coefficient calculated by the interpolation function ( $C_{My,fit}$ ). The black triangular points represent the yawing coefficient  $C_{Mz}$  calculated by direct simulation ( $C_{Mz,sim}$ ), and the black dashed line represents the yawing coefficient calculated by the interpolation function ( $C_{Mz,fit}$ ). The interpolation functions of the aerodynamic moment coefficients are determined as follows:

$$C_{Mx} = -0.2493\psi_w^4 + 0.1436\psi_w^3 + 0.359\psi_w^2 + 0.7475\psi_w \quad (35)$$

$$C_{My} = -2.95\psi_w^4 + 10.38\psi_w^3 - 11.55\psi_w^2 + 3.835\psi_w - 0.129 \quad (36)$$

$$C_{Mz} = 1.592\psi_w^4 - 3.752\psi_w^3 - 4.756\psi_w^2 + 9.872\psi_w \quad (37)$$

The interpolation functions to calculate the coefficients  $C_{Mx}$ ,  $C_{My}$ ,  $C_{Mz}$  also have R-square indexes of approximately 0.99. The results in Fig. 7 show that the rolling coefficient reaches the maximum value  $C_{Mx,max} = 1.19$  at  $\psi_w = 75^\circ$ . The pitching coefficient reaches the maximum value  $C_{y,max} = 0.26$  at  $\psi_w = 22^\circ$ . The yawing coefficient reaches the maximum value  $C_{Mz,max} = 3.68$  at  $\psi_w = 40^\circ$ .

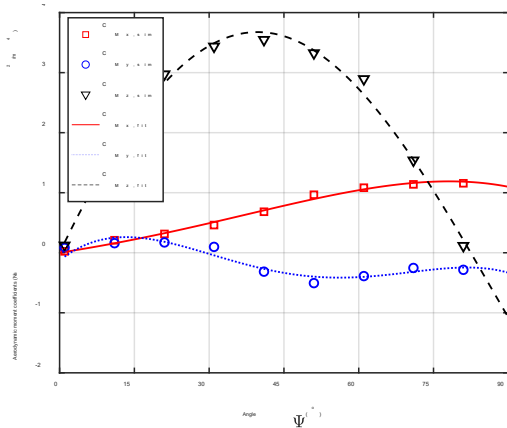


Fig. 7. Aerodynamic moment coefficients

The results in Fig. 7 also show that, when the

crosswind has a direction almost perpendicular to the side of the body ( $\psi_w > 75^\circ$ ), the yawing moment coefficient ( $C_{Mz}$ ) is negative, that is, when the center of the crosswind side is located behind the vehicle's center of gravity (along the  $x$ -axis). The reason for this phenomenon is because the body of the vehicle in the aerodynamic simulation has been assumed to be a solid block, so when the angle  $\psi_w$  changes, the resistance area (depending on the body size) of the bus also changes. The change of the yawing moment  $M_{wz}$  depends on the drag force (along the  $x$ -axis) and the side force (along the  $y$ -axis). In cases where the angle  $\psi_w$  is close to  $90^\circ$ , the  $C_{Mz}$  coefficient is negative because the side force  $F_{wy}$  ( $C_y$  coefficient) decreases from its maximum value, and the drag force  $F_{wx}$  ( $C_x$  coefficient) is negative in this case (Fig. 6).

**4.2. Evaluation of Bus Instability in Static Crosswind Conditions**

This study evaluated the bus instability in static crosswind conditions by determining the limiting speeds for the unstable states presented in section 3. In this study, the crosswind is characterized by the change of wind speed, while the wind direction is perpendicular to the side surface of the bus ( $\psi_w = 90^\circ$ ). The limits of the bus speed and the wind speed are both 200 km/h. In addition, with different vehicle speeds and crosswind speeds, using formulas (12) and (13) we can calculate the equivalent wind parameters. From there, the corresponding aerodynamic coefficients are selected thanks to the results shown in Fig. 6 and 7. The vehicle characteristics used in the calculation are presented in Table 2.

Table 2. Vehicle parameters

Parameter	Unit	Value
$m$	kg	12500
$a$	m	3.69
$b$	m	2.46
$c$	m	2.5
$h$	m	1.5
$A$	m <sup>2</sup>	8.2769
$f$		0.02
$\mu$		0.5

Using the numerical calculation method, we have calculated and determined the limit speeds that cause bus instability when moving in crosswind conditions.

Fig. 8 shows the limit speeds for the types of instability: loose contact of the front wheel 11 (blue dashed line with circle point), loose contact of rear wheel 21 (blue solid line with square point), sideslip of front wheels (red dashed line with diamond point), and slide of the rear wheel (red solid line with triangle point). Each line of the limit speed divides the graph

plane into two zones: the lower left is the stability zone, the upper right is the instability zone. Based on the limit speeds line, we can find out the wind speed that causes instability according to the bus speed.

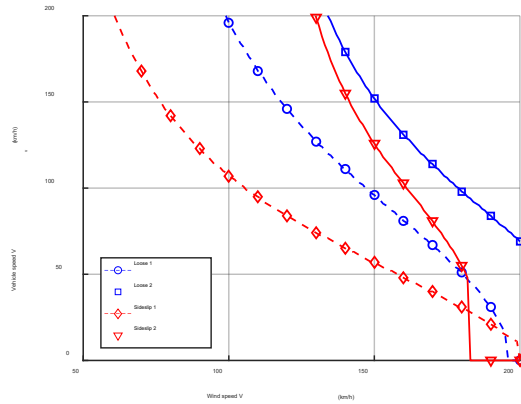


Fig. 8. Graph of limit speeds causing bus instability

Consider the phenomenon of loss of contact between the wheel and the road surface and the phenomenon of rollover: the results in Fig. 8 show that, with a 45-seat bus, when the wind speed increases, wheel 11 (front axle) loses contact with the road before wheel 21 (rear axle) loses contact. Thus, the limit speed of the vehicle on the left side (on the same side of the crosswind) is equal to the speed limit when wheel 21 loses contact with the road.

Considering the phenomena of body rotation and side slippage: The results in Fig. 8 show that, when the vehicle moves at a low speed (< 30 km/h), and the wind speed is more significant than 182 km/h, the rear wheels will sideslip before the front wheels. In this case, the bus tends to rotate around the front axle. When the vehicle moves at a speed greater than 30 km/h, and the wind speed increases, the front wheels will be sideslip before the rear wheels. In this case, the bus tends to rotate around the rear axle. The results also showed that the bus slide completely (all four wheels sideslip), mainly when the rear wheels are sideslip.

Table 3. Limit speeds do not cause instability in some cases of vehicle speed

Instability	Bus speed (km/h)		
	80	100	120
Sideslip of front wheels	124	106	92
Sideslip of rear wheels	170	160	152
Loss of wheel 11	161	144	134
Loss of wheel 21	192	179	166

The values of the limit wind speed that do not cause instability (loss of wheels 11 and 21, sideslip of

front and rear wheels) in bus speed of 80 km/h, 100 km/h, and 120 km/h are summarized in Table 3. The results show that with the aerodynamic shape of this bus, dangerous instability is concentrated on the front axle. Therefore, the aerodynamic design of the car needs special attention because the front axle is the driving guide, which is more likely to cause an accident.

## 5. Conclusion

The paper presents the following main results:

- Determination of the polynomial interpolation functions to calculate the aerodynamic coefficients of the bus. These interpolation functions can be used in bus dynamics simulation in crosswind conditions;
- Determination of the value of speed causing instability (rollover, sideslip, loss of contact) according to the dimensions and aerodynamic characteristics of the bus body;
- Construction of a graph of the relationship between the bus speed and the wind speed to determine the limit wind speeds to not cause instability for the bus.

However, the studies were only carried out in the case of the vehicle moving in a straight line in static crosswind conditions. This study did not take into account the influence of suspension and tire stiffness, nor did it evaluate the instability of the bus trajectory on the road. A complete study of bus dynamics will need to be developed in the future in order to better evaluate the effect of crosswinds on bus stability during actual motion.

## Acknowledgments

This research is funded by the Hanoi University of Science and Technology (HUST) under grant number T2018-PC-046.

## References

- [1] W.H. Hucho, *Aerodynamics of Road Vehicles*. Butterworth Ltd., London, England 1987.
- [2] C.J. Baker, A simplified analysis of various types of wind-induced road vehicle accidents, *J. Wind Eng. Ind. Aerodyn.* Vol. 22(1), pp.69-85, 1986. [https://doi.org/10.1016/0167-6105\(86\)90012-7](https://doi.org/10.1016/0167-6105(86)90012-7)
- [3] C.J. Baker, High sided articulated road vehicles in strong cross winds. *J. Wind Eng. Ind. Aerodyn.* Vol. 31, pp. 67–85, 1988. [https://doi.org/10.1016/0167-6105\(88\)90188-2](https://doi.org/10.1016/0167-6105(88)90188-2)
- [4] W.H. Guo, Y.L. Xu, Dynamic analysis of moving road vehicle under a sudden crosswind. *Key Eng. Mater.* Vol. 243–244, pp. 141–146, 2003. <https://doi.org/10.4028/www.scientific.net/KEM.243-244.141>
- [5] M. Batista, M. Perkovič, A simple static analysis of moving road vehicle under crosswind, *J. Wind Eng. Ind. Aerodyn.* Vol. 128, pp. 105–113, 2014.

- <https://doi.org/10.1016/j.jweia.2014.02.009>
- [6] Z. Zhang, J. Li, W. Guo, Combined simulation of heavy truck stability under sudden and discontinuous direction change of crosswind with computational fluid dynamics and multi-body system vehicle dynamics software, *Advances in Mechanical Engineering* Vol. 10, pp. 1-10, 2018.  
<https://doi.org/10.1177/1687814018786364>
- [7] T.D. Gillespie, *Fundamentals of Vehicle Dynamics*. SAE Inc., Warrendale, PA, 1992.  
<https://doi.org/10.4271/R-114>
- [8] T.H. Tung, Research for improvement the aerodynamic shape of coach assembled in Vietnam, Ph.D. dissertation, Hanoi University of Science and Technology, 2016.
- [9] D.T. Quyet, N.T. Hoan, T.M. Hoang, Study on computation of aerodynamic force acting on bus in crosswind conditions by using CFD, *The First International Conference on Fluid Machinery and Automation Systems ICFMAS2018*, Hanoi, Vietnam, pp. 522-527, 2018.
- [10] D.T. Quyet, N.T. Hoan, T.M. Hoang, Determining aerodynamic forces acting on the bus by experiment, *Vietnam Mechanical Engineering Journal*, Vol. 10, pp.406-411, 2020.